

The value of the activation volume for nitrogen is considerably smaller than that for oxygen. On the basis of the ionic radii of the interstitial atoms alone, one might expect nitrogen to show a larger effect, since the nitrogen and oxygen ionic radii are 1.71 Å and 1.40 Å, respectively. However, any chemical affinity between oxygen and the vanadium atoms may cause the interstitial volume to be effectively larger for oxygen than for nitrogen.

The present results are in sharp distinction to those obtained by Bosman, Brommer, and Rathenau<sup>7,8</sup> in the analogous  $\alpha$ -iron-nitrogen and  $\alpha$ -iron-carbon systems. The activation volumes for interstitial oxygen and nitrogen in vanadium are apparently much larger than for nitrogen in iron, the value for oxygen being forty times larger and the value for nitrogen being thirty times larger. For carbon in  $\alpha$ -iron, Bosman,

Brommer, and Rathenau obtain a negative activation volume. At present, the reasons for this discrepancy are completely obscure. However, neither the present measurement nor that of Bosman *et al.* involve direct measurements of diffusion; possibly the processes are somewhat more complicated than generally supposed. It is hoped that this situation may be clarified by additional experiments.

#### ACKNOWLEDGMENT

The authors wish to express their sincere thanks to Professor C. A. Wert for suggesting the suitability of the vanadium-oxygen and vanadium-nitrogen systems, and for his kindness in providing the vanadium samples. The authors also wish to thank Mr. James Boyd for assistance in making some of the measurements.

## Electron Effective Masses of InAs and GaAs as a Function of Temperature and Doping

MANUEL CARDONA

Laboratories RCA Ltd., Zurich, Switzerland

(Received September 19, 1960)

The electron effective masses of several GaAs and InAs samples at room and liquid nitrogen temperatures have been determined from Faraday rotation and infrared reflectivity measurements. An increase in effective mass with increasing carrier concentration has been found in both materials. This increase can be quantitatively interpreted in InAs in terms of the nonparabolic nature of the conduction band. In GaAs the increase in effective mass with doping suggests the existence of another set of conduction band minima above the lowest (000) minimum. The measured temperature variation of the effective mass can be attributed to two mechanisms: the increase in effective mass produced by the spread in the Fermi distribution because of the nonparabolic shape of the band, and the variation in the band structure produced by the thermal expansion of the lattice.

The Faraday rotation due to the interband transitions has been measured in GaAs and InAs. This rotation is clockwise along the direction of motion of the radiation and the magnetic field for GaAs and counterclockwise for InAs. This effect is compared with the corresponding effect in other semiconductors.

### 1. INTRODUCTION

THE variation of the electron effective mass with temperature found experimentally in Ge<sup>1,2</sup> has been interpreted as due to the slight nonparabolicity of the energy band and the variation of the corresponding energy gap with volume.<sup>1</sup> The temperature variation of the effective mass produced by the nonparabolicity of the band and the one due to the change of the energy gap have opposite signs for the III-V semiconductors with a lowest (000) conduction band minimum. Hence, a very small variation of the effective mass with temperature should be expected for these semiconductors. This conclusion has been experimentally confirmed by the author, who found a temperature variation smaller than

2% between 80 and 297°K in the electron effective mass of GaAs and InP as determined from the infrared reflectivity of these materials.<sup>3</sup>

A large increase in the electron effective mass of InSb with increasing carrier concentration has been found by several authors.<sup>4,5</sup> This effect can be explained in terms of the strong nonparabolic character of the conduction band of this material, produced by the small energy gap. A somewhat smaller effect should be expected for InAs and a much smaller one for GaAs.

In this paper, infrared reflectivity and Faraday rotation measurements on InAs and GaAs at several temperatures and dopings are reported. The electron effective

<sup>3</sup> M. Cardona, to be reported at the Prague Conference on Semiconductors, August-September, 1960.

<sup>4</sup> W. G. Spitzer and H. Y. Fan, Phys. Rev. **106**, 882 (1957).

<sup>5</sup> S. D. Smith, T. S. Moss, and K. W. Taylor, J. Phys. Chem. Solids **11**, 131 (1959).

<sup>1</sup> M. Cardona, W. Paul, and H. Brooks, Helv. Phys. Acta (to be published).

<sup>2</sup> D. Geist, Z. Physik **137**, 335 (1959).

masses derived from these measurements are compared with the theoretical predictions. Also the Faraday rotation produced by the interband transitions in these materials is compared with the corresponding effect in other semiconductors.

## 2. EXPERIMENTAL METHOD

### (a) Faraday Rotation Measurements

The optical set up used for Faraday rotation measurements can be seen in Fig. 1. A Leiss single monochromator with a quartz or a KBr prism was used to obtain monochromatic radiation. The radiation from a globar was chopped at 13 cps. A Reeder radiation thermocouple with KRS-5 window was used with the KBr prism and a PbS photocell with the quartz prism. A set of two spherical and one plane mirror produced a parallel beam which was polarized by means of a Glan-Thompson prism in the quartz region and by two parallel germanium plates in the KBr region. The germanium plates polarized by transmission at the Brewster angle ( $76^\circ$ ). The theoretical degree of polarization produced by each plate was 88%. A transmission polarizer was used instead of a reflection one to simplify the collimation problem. The radiation passed through the drilled plane pole pieces of a Newport magnet. The diameter of the hole was 1.6 cm and hence the available aperture was fairly small. The samples were placed inside a cryostat between the pole pieces of the magnet with a 2-cm gap. The analyzer was slowly rotated by means of a motor; a notched wheel with 36 notches produced, in conjunction with a microswitch, a mark on an  $x-t$  recorder each  $10^\circ$  of rotation. The transmitted energy was amplified and recorded as a function of the analyzer angle. The position of the maxima or minima was determined to  $\pm 0.5^\circ$  from several pairs of symmetrical points.

The samples were ground and polished with Linde A-5175 and B-5125 polishing compounds. They were held against a copper block in the cryostat by means of a spring. The temperature was measured with a copper-constantan thermocouple soldered to the spring and held against the sample.

The Hall constants were determined at room temperature on bars cut from the optical samples after the optical measurements had been performed. Low-resistivity contacts were placed on InAs by means of silver paste and on GaAs by the method of Willardson and Duga.<sup>6</sup> Indium was soldered to the sample after etching in a mixture of 1 part of HCl and 1 part of  $\text{HNO}_3$  and rinsing in distilled water. The use of ultrasonics was not found necessary for the soldering. The sample was then baked for 1 hour at  $250^\circ\text{C}$  in an argon atmosphere. The carrier concentration was calculated for all samples assuming the ratio of Hall to conductivity mobility equal to one. It has been shown by Ehrenreich<sup>7</sup> that this ratio

<sup>6</sup> R. K. Willardson and J. J. Duga, Proc. Phys. Soc. (London) 75, 280 (1960).

<sup>7</sup> H. Ehrenreich, J. Phys. Chem. Solids 9, 129 (1959).

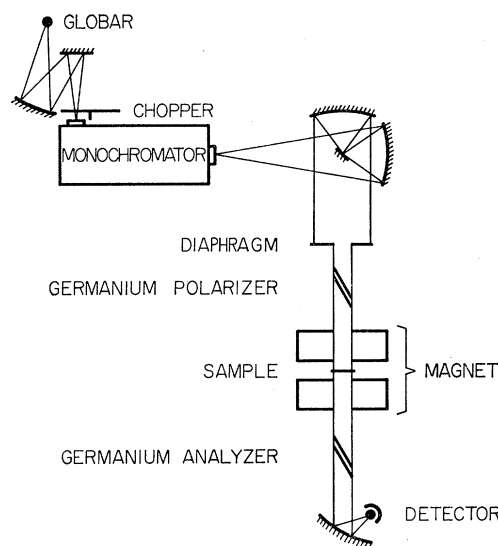


FIG. 1. Optical setup used for Faraday rotation measurements.

lies between 1 and 1.1 for intrinsic InSb. With increasing degeneracy of the statistics, this ratio will deviate less from one. For InAs and GaAs the mobility ratio should not significantly differ from the ratio for InSb. The error introduced by assuming the ratio of these mobilities equal to 1 will be smaller in the Faraday rotation measurements where  $m^*$  is proportional to the carrier concentration  $N$ .

### (b) Reflectivity Measurements

The method used for the reflectivity measurements has been described elsewhere.<sup>1</sup> The reflectivity was determined by comparison with the reflectivity of intrinsic germanium. One of the sides of the sample was optically polished and the sample placed inside an optical cryostat with one KBr window. The reflectivity was measured at an angle of incidence of  $5^\circ$ . Under these circumstances, the measured reflectivity differs from the reflectivity for normal incidence by an amount much smaller than the experimental error.

## 3. RESULTS

### (a) GaAs

The Faraday rotation as a function of wavelength was measured on two  $n$ -type GaAs samples. The sample with a carrier concentration  $N = 2.36 \times 10^{18} \text{ cm}^{-3}$  was measured for wavelengths between 1 and 2.8 microns with quartz optics. The other sample, carrier concentration  $N = 1.48 \times 10^{17} \text{ cm}^{-3}$ , was measured between 1 and 10 microns with KBr optics. Both samples were 0.83 mm thick. The linearity of the rotation as a function of magnetic field  $B$  was checked at a fixed wavelength. The measurements as a function of wavelength were performed at a fixed value of  $B = 8330$  gauss and for two opposite directions of  $B$ .

Figure 2 shows the Faraday rotation observed in the GaAs sample with  $N=2.36 \times 10^{18} \text{ cm}^{-3}$  as a function of the square of the wavelength and at two different temperatures (296 and 98°K). At wavelengths above 1.7  $\mu$ , the rotation increases linearly with the square of the wavelength; it seems reasonable to assign this rotation to the free electrons in the conduction band. All the effective-mass determinations have been made from the slope of the linear part of these curves by using the formula<sup>5</sup>:

$$m_{op}^* = \left\{ \frac{e^3}{8\pi^2 c^3 \epsilon_0} \right\}^{\frac{1}{2}} \lambda \left( \frac{BN}{n\theta} \right)^{\frac{1}{2}}, \quad (1)$$

where mks units are used,  $e$  is the elementary charge,  $c$  is the speed of light,  $\lambda$  is the wavelength,  $\epsilon_0$  is the dielectric constant of vacuum,  $n$  is the refractive index of the material, and  $\theta$  is the rotation per unit length (in rad/m).

When approaching the energy gap, the rotation increases very rapidly. This contribution to the rotation must be produced by the interband transitions. The difference between the rotation at room temperature and at 98°K was fitted by the least-squares method. From this fit and after correcting for the variation of  $n$  with temperature,<sup>3</sup> we find that, between 98 and 297°K,  $\Delta m^* = -(1 \pm 3)\%$ . The calculated value of the optical effective mass is  $m_{op}^* = (0.083 \pm 0.005)m$ . This sample is degenerate at room temperature so that no error is introduced by assuming a ratio of Hall to conductivity mobility equal to one. The error in  $m^*$  stems from the error in the determination of  $\theta$  and the error in the determination of the Hall constant.

Figure 3 shows the Faraday rotation produced by the GaAs sample with  $N=1.48 \times 10^{17} \text{ cm}^{-3}$  at room temperature and at 100°K. The rotation produced by the interband transitions is similar to the one produced by the other GaAs sample. From the free-carrier effect, the effective mass  $m_{op}^* = 0.067m$  is found. This value is affected by a  $\pm 2\%$  error produced by the inaccuracy of the Hall measurement and the assumption the ratio of Hall to conductivity mobility is equal to one. The

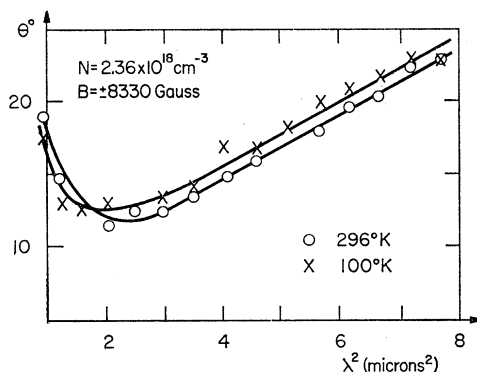


FIG. 2. Faraday rotation produced by an  $n$ -type GaAs sample as a function of the square of the wavelength.

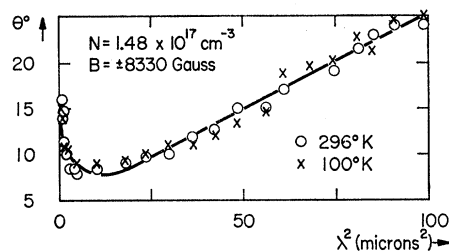


FIG. 3. Faraday rotation in an  $n$ -type GaAs sample as a function of the square of the wavelength.

difference between the rotation at room temperature and at 100°K, fitted by the least-squares method, yields an increase in  $m^*$  of  $(2 \pm 2)\%$  between 100 and 296°K.

### (b) InAs

Two InAs samples were measured. One of them had a carrier concentration  $N=4.9 \times 10^{16} \text{ cm}^{-3}$ , and a thickness of 1.92 mm. Its Faraday rotation was measured between 5 and 10 microns with KBr optics. The other sample, carrier concentration  $5.17 \times 10^{18} \text{ cm}^{-3}$ , was measured by the reflectivity method, as Faraday rotation could not be observed due to the high absorption coefficient. Figure 4 shows the Faraday rotation produced by the first sample in a field of  $\pm 8330$  gauss as a function of the square of the wavelength. In contrast to GaAs, the Faraday rotation produced by the interband transitions in InAs is opposite to the effect of the free electrons.

An increase in the slope of the linear part of the curves with decreasing temperature can be clearly observed. The difference between the rotations at 100°K and at 296°K, fitted by the least-squares method and corrected for the variation of the refractive index with temperature,<sup>3</sup> yields an increase in  $m^*$  with increasing temperature of  $5 \pm 1\%$  between 100 and 296°K. The effective mass at room temperature calculated by means of Eq. (1) is  $m_{op}^* = 0.027m$ . This value is affected by an error of  $\pm 1\%$  due to the error in the measurement of  $\theta$  and  $(+7, -2)\%$  error due to the inaccuracy in the measurement and interpretation of the Hall constant. The total error is thus  $(+8, -3)\%$ .

Figure 5 shows the reflectivity of InAs with  $N=5.17 \times 10^{18} \text{ cm}^{-3}$  at 296 and 100°K. Figure 6 shows the dielectric constant  $\epsilon$  (with respect to the vacuum) calculated from the reflectivity as a function of the square of the wavelength. The effective mass can be found from these data by means of the equation (in mks units):

$$\epsilon = \epsilon_i - \frac{e^2 N}{\epsilon_0 \omega^2 m_{op}^*}, \quad (2)$$

where  $\epsilon_i$  is the dielectric constant of the intrinsic material with respect to the vacuum. We obtain for the material under consideration  $m_{op}^* = (0.052 \pm 0.005)m$ .

The difference between the dielectric constant at 296°K and 100°K, fitted as a function of the square of

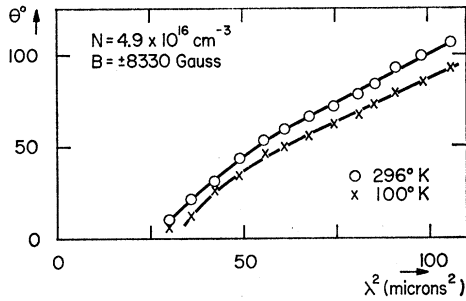


FIG. 4. Faraday rotation produced by an *n*-type InAs sample as a function of the square of the wavelength.

the wavelength by the least-squares method, gives a  $(1 \pm 1.6)\%$  decrease in  $m_{op}^*$  with increasing temperature.

#### 4. DISCUSSION

##### (a) Interband Faraday Rotation

It has been shown in Sec. 3 that the Faraday rotations produced by the interband polarizability in GaAs and InAs have opposite signs. For GaAs this rotation has the same sign as the free electron rotation. The interband Faraday rotation has also been measured for GaP, Si, InP,<sup>8</sup> InSb,<sup>5</sup> and Ge.<sup>9</sup> In all except InSb the rotation has the same sign as the free electron rotation. This effect can be easily understood for nondegenerate valence and conduction bands<sup>10</sup> (not the real case). In this case, the levels in each band coalesce into two ladders of Landau levels corresponding to the two possible spin orientations. Each ladder has infinite levels characterized by the quantum number  $l=0, 1, 2, \dots$  (see Fig. 7). The distance between the levels in both ladders corresponding to the same  $l$  number is determined by the effective  $g$  factor of the band. In Fig. 7 both  $g$  factors have been taken positive. Under these conditions, the only transitions allowed are these for which  $\Delta l=0$  and  $\Delta J_z = \pm 1$ ;  $\Delta J_z = +1$  corresponds to circularly polarized radiation clockwise along the direction of motion of the radiation and  $\Delta J_z = -1$  corresponds to the counterclockwise polarization. Figure 7 shows that for the counterclockwise polarization the transitions occur at smaller energies than for the clockwise polarization and a larger polarizability for these transitions should be expected at energies smaller than the energy gap (the probabilities are the same for both transitions). Hence a clockwise rotation will result (the free electron rotation is also clockwise). If both  $g$  factors were negative, we should have found a counterclockwise rotation. For a positive and a negative  $g$  factor, a compensation occurs and the sense of the rotation is determined by the largest  $g$  factor. Actually the valence band at  $k=0$  is fourfold degenerate in the absence of a magnetic field and the above considerations cannot be applied rigor-

<sup>8</sup> H. Kimmel, Z. Naturforsch. **12**, 1016 (1957).

<sup>9</sup> A. K. Walton and T. S. Moss, J. Appl. Phys. **30**, 951 (1959).

<sup>10</sup> E. Burstein, G. S. Picus, R. F. Wallis, and F. Blatt, Phys. Rev. **113**, 15 (1959).

ously. Exact calculations would only be possible in the case of germanium where the valence band energy levels in the presence of a magnetic field and the matrix elements for the optical transitions have been calculated.<sup>10</sup> The  $g$  factor of the conduction band in germanium is  $-3$ .<sup>10</sup> Hence, to explain the clockwise rotation found experimentally, we must conclude that the valence band behaves as a nondegenerate band with a positive  $g$  factor. The same thing must be true for all other semiconductor for which clockwise interband rotation has been observed. For InAs and InSb the  $g$  factors are  $-32$  and  $-54$ , respectively; the effect of these large negative  $g$  factors is dominant and a counterclockwise rotation is observed.

##### (b) Free-Carrier Effect in GaAs

The conduction band of a semiconductor around the (000) minimum, considering only the interaction between this minimum and the valence band maximum, is given by the solution of<sup>11</sup>

$$E'(E'+2\Delta)(E'+E_s+2\Delta) - k^2\beta^2(E'+\frac{2}{3}E_s+2\Delta) = 0, \quad (3)$$

where the energy  $E = E' + (\hbar^2 k^2 / 2m)$ ,  $\mathbf{k}$  is the crystal momentum,  $2\Delta$  is the energy gap,  $\beta^2$  is the square of the matrix element of the linear momentum between conduction and valence band at  $k=0$ , and  $E_s$  is the spin-orbit splitting. For the GaAs samples under consideration  $E' \approx E$ ,  $E \ll 2\Delta$ , and  $E_s \ll 2\Delta$ ; hence from (3) we obtain

$$E \approx -\Delta + (\Delta^2 + k^2\beta^2)^{1/2}. \quad (4)$$

For the energy bands given by Eq. (4) it is possible to show that the Faraday rotation effective mass defined by Eq. (1) and the reflectivity effective mass defined by Eq. (2) are identical and given by the expression (see

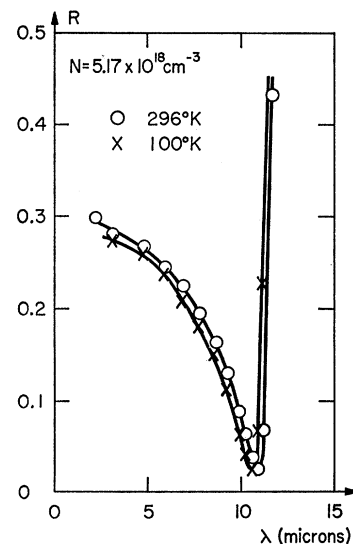


FIG. 5. Reflectivity in an *n*-type InAs sample as a function of the wavelength.

<sup>11</sup> E. O. Kane, J. Phys. Chem. Solids **1**, 249 (1957).

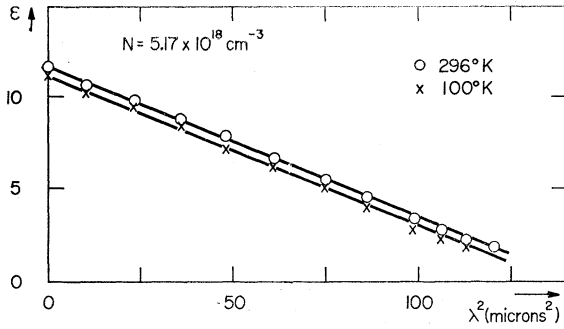


FIG. 6. Dielectric constant of an  $n$ -type InAs sample as a function of the square of the wavelength.

Appendix):

$$\frac{1}{m_{op}^*} = \frac{1}{m^*} \left[ 1 - \frac{5 kT}{3 \Delta} \frac{\int_0^\infty x^3 f(x-\eta) dx}{\int_0^\infty x^3 f(x-\eta) dx} \right], \quad (5)$$

where  $m^*$  is the effective mass at the bottom of the band,  $k$  is the Boltzmann constant,  $f$  is the Fermi function, and  $\eta = E_F/kT$ , where  $E_F$  is the Fermi energy. The Fermi energy  $E_F$  can be found from

$$N = \frac{\sqrt{2}(kT)^{3/2} m^{*3/2}}{\pi^2 \hbar^3} \times \left[ \int_0^\infty x^3 f(x-\eta) dx + \frac{5 kT}{4 \Delta} \int_0^\infty x^3 f(x-\eta) dx \right]. \quad (6)$$

For completely degenerate statistics, Eq. (5) becomes

$$\frac{1}{m_{op}^*} = \frac{1}{m^*} \left[ 1 - \frac{E_F}{\Delta} \right]. \quad (7)$$

Figure 8 shows the values of the effective mass in  $n$ -type material found by Moss,<sup>12</sup> Spitzer and Whelan,<sup>13</sup> and ourselves as a function of the position of the Fermi level at 0°K. Some of these effective masses were measured at room temperature, but their temperature coefficient was shown in Sec. 3 to be very small so that we can assume the points in Fig. 8 to be the effective masses at 0°K. The broken line in Fig. 8 has the slope of Eq. (7). The solid line is the least-squares fit to the experimental points. The agreement between the theoretical and the experimental line is good within the probable error of the least-squares fit.

For the temperature increase in the effective mass produced by the nonparabolicity of the band, Eq. (5) yields 5.7% for the sample with  $N = 1.48 \times 10^{17} \text{ cm}^{-3}$  and 4.8% for the sample with  $N = 2.36 \times 10^{18}$ . From these increments we have to subtract the decrease in the effective mass produced by the thermal expansion of the

lattice.<sup>14,15</sup> This effect can be estimated by assuming that the matrix element  $\beta$  is constant. Differentiating  $m^* = \hbar^2 \Delta / \beta^2$ , we get

$$\frac{dm^*}{m^*} = \frac{d\Delta}{\Delta} = \left[ \left( \frac{\partial \Delta}{\partial p} \right)_T \frac{1}{V} \left( \frac{\partial V}{\partial T} \right)_P / \frac{1}{V} \left( \frac{\partial V}{\partial p} \right)_T \right] \frac{dT}{\Delta}, \quad (8)$$

where  $V$  is the volume,  $p$  is the applied pressure,  $(1/V)(\partial V/\partial p)_T$  is the compressibility of the material<sup>14</sup>  $= 1.32 \times 10^{-6} \text{ cm}^2/\text{kg}$ ,  $(1/3V)(\partial V/\partial T)_P$  is the linear thermal expansion coefficient<sup>16</sup>  $= 5.7 \times 10^{-6} (\text{°C})^{-1}$ , and  $(\partial \Delta/\partial p)_T = 7 \times 10^{-6} \text{ eV} \times \text{cm}^2/\text{kg}$ .<sup>17</sup> The calculated effect between 100 and 296°K is a decrease in  $m^*$  of 2.5%.

A net increase in  $m_{op}^*$  between 100 and 296°K of 3.2% should thus be observed for  $N = 1.48 \times 10^{17} \text{ cm}^{-3}$  and an increase of 2% for  $N = 2.36 \times 10^{18}$ . These values are in good agreement with the experimental ones described in Sec. 3.

### (c) Free Carrier Effect in InAs

The approximations  $E \ll 2\Delta$  and  $E_s \ll 2\Delta$  introduced in Eq. (3) for GaAs are not valid in general for InAs. For the measured material, however,  $E < 2\Delta + \frac{2}{3}E_s$  and we can write in first approximation:

$$E = -\Delta + (\Delta^2 + k^2 \gamma^2)^{1/2}, \quad \text{with} \quad \gamma^2 = \beta^2 \frac{2\Delta + \frac{2}{3}E_s}{2\Delta + E_s}, \quad (9)$$

which is similar to Eq. (4). A second order correction to Eq. (9) can be found for  $k^2 \gamma^2 \ll \Delta^2$  by expanding Eq. (3) in a power series of  $k^2 \gamma^2 / \Delta^2$ . We get

$$E = \frac{\gamma^2}{2\Delta} k^2 - \frac{\gamma^4}{8\Delta^3} (1 - 2A\Delta) k^4, \quad (10)$$

$$A = \frac{1}{2\Delta + \frac{2}{3}E_s} \frac{1}{2\Delta + E_s}.$$

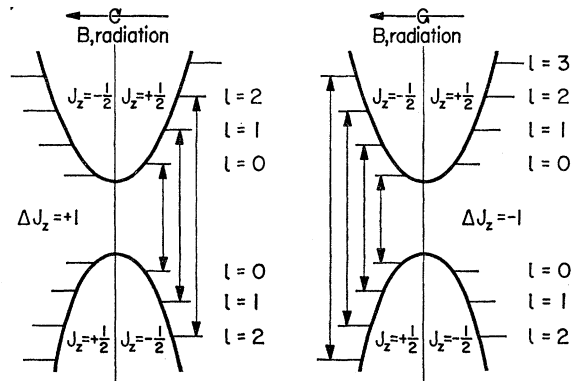


FIG. 7. Energy levels and allowed transitions for nondegenerate energy bands with positive  $g$  factors with an applied magnetic field along the direction of the incident radiation.

<sup>14</sup> J. C. Phillips, Phys. Rev. **113**, 147 (1959).

<sup>15</sup> J. Callaway, J. Electron. **2**, 330 (1957).

<sup>16</sup> H. Welker, in *Solid-State Physics*, edited by F. Seitz and D. Turnbull (Academic Press, New York, 1956), Vol. III, p. 51.

<sup>17</sup> D. M. Warschauer and W. Paul (private communication).

<sup>12</sup> T. S. Moss and A. K. Walton, Proc. Phys. Soc. (London) **74**, 131 (1959).

<sup>13</sup> W. G. Spitzer and J. M. Whelan, Phys. Rev. **114**, 59 (1959).

For InAs,  $2A\Delta \approx 0.1$ . We can take care of this correction by using Eq. (9) with an effective energy gap 10% larger than the real one. Thus, for  $E_F \ll \Delta$  (sample with  $N = 4.9 \times 10^{16} \text{ cm}^{-3}$ ), Eq. (5) can be used with 10% higher than the corresponding value for InAs. When  $E_F$  is not much smaller than  $\Delta$  (sample with  $N = 5.17 \times 10^{18} \text{ cm}^{-3}$ ), this series expansion is not usable and Eqs. (4) and (5) are not valid. One can, however, find a simple exact expression for  $N$  and  $m^*$  at 0°K for the approximate energy band of Eq. (9). Substituting Eq. (9) into (11):

$$\frac{1}{m_{op}^*} = \frac{\int \nabla_k^2 E f(E - E_F) d\mathbf{k}}{3\hbar^2 \int f(E - E_F) d\mathbf{k}}, \quad (11)$$

$$N = \frac{1}{4\pi^3} \int f(E - E_F) d\mathbf{k},$$

one finds exactly at 0°K:

$$\frac{1}{m_{op}^*} = \frac{\gamma^2}{E_F + \Delta}, \quad N = \frac{E_F^{\frac{3}{2}}(E_F + 2\Delta)^{\frac{3}{2}}}{3\pi^2 \gamma^3}. \quad (12)$$

In this case one can also calculate the variation of  $m_{op}^*$  with temperature for  $E_F \gg kT$  by using the expansion<sup>18</sup>:

$$-\int_0^\infty \phi(E) \frac{\partial f}{\partial E} dE \approx \phi(E_F) + \frac{\pi^2}{6} (kT)^2 \left( \frac{d^2 \phi}{dE^2} \right)_{E_F} + \dots, \quad (13)$$

where  $\phi$  is an arbitrary function of the energy.

Figure 9 shows the effective mass of InAs found by Spitzer and Fan<sup>4</sup> and the values reported in this work as a function of carrier concentration. The solid curve

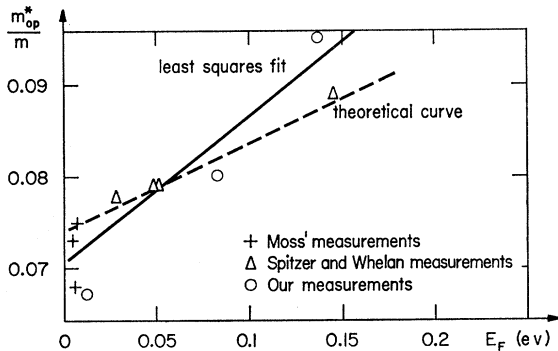


FIG. 8. Effective mass of  $n$ -type GaAs as a function of the position of the Fermi level.

<sup>18</sup> A. H. Wilson, *The Theory of Metals* (Cambridge University Press, New York, 1954), p. 13.

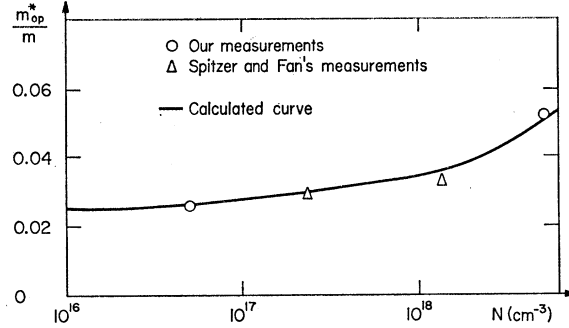


FIG. 9. Effective mass of  $n$ -type InAs as a function of the carrier concentration.

has been calculated by using Eq. (12) and the value of  $m_{op}^*$  found for  $N = 4.9 \times 10^{16} \text{ cm}^{-3}$ .

For  $N = 4.8 \times 10^{16} \text{ cm}^{-3}$  Eq. (6) yields a 16% increase in  $m^*$  between 100 and 296°K. To calculate the effect produced by the thermal expansion we assume that the compressibility of InAs is  $7 \times 10^{-7} \text{ cm}^2/\text{kg}$ , the average between the compressibilities of InSb and Ge, as no experimental data for InAs have been found in the literature. If the pressure coefficient of the energy gap is taken to be  $1.5 \times 10^{-5} \text{ eV} \times \text{cm}^2/\text{kg}$ , the same as for InSb,<sup>19,20</sup> one finds a decrease of 8% in  $m^*$  between these temperatures. This yields a net increase of 8% with increasing temperature which, considering the inaccuracy of the above estimate, is in reasonable agreement with the 5% found experimentally.

For the InAs sample with  $N = 5.17 \times 10^{18} \text{ cm}^{-3}$ , the nonparabolic effect can be calculated by using Eq. (13). The effective mass increases with temperature because of the spread in the Fermi distribution but also decreases because of the lowering of the Fermi level. The net calculated effect is smaller than 1%. The effect of the thermal expansion can be calculated from Eq. (12) taking into account the  $\Delta$  dependence of  $\gamma$  given by Eq. (9). A 2% decrease in  $m^*$  between 100 and 296°K is found. This value reasonably agrees with the experimental value reported in Sec. 3.

#### ACKNOWLEDGMENTS

The author wants to express his gratitude to the staff of the Laboratories RCA Ltd., for innumerable discussions and suggestions. The samples used for these measurements were supplied by the RCA Laboratories of Princeton, New Jersey. The optical samples were skilfully prepared by Mr. Heinrich Meier, who also contributed to setting up the equipment.

#### APPENDIX

The free-carrier polarizability for arbitrary energy surfaces can be calculated from Eq. (11). For spherical energy surfaces the integral which appears in the

<sup>19</sup> W. Paul, *J. Phys. Chem. Solids* **8**, 196 (1959).

<sup>20</sup> D. Long, *Phys. Rev.* **99**, 388 (1955).

numerator of Eq. (11) can be written:

$$\int \nabla_{\mathbf{k}}^2 E f(E - E_F) d\mathbf{k} = 4\pi \int_0^\infty \frac{d}{dE} \left( k^2 \frac{dE}{dk} \right) f(E - E_F) dE, \quad (\text{A1})$$

where  $k$  is the magnitude of  $\mathbf{k}$ . Under the same assumption the carrier density becomes:

$$N = \frac{1}{4\pi^3} \int f(E - E_F) d\mathbf{k} = \frac{1}{\pi^2} \int_0^\infty k^2 f(E - E_F) dk. \quad (\text{A2})$$

Let us assume that the energy can be expanded in power series of  $k$  as follows:

$$E = Ak^2 + B'k^4 + \dots \quad (\text{A3})$$

By substituting Eq. (A3) into Eq. (A1) and neglecting all powers of  $k$  higher than  $k^4$ , we find

$$\int \nabla_{\mathbf{k}}^2 E f(E - E_F) d\mathbf{k} = \int_0^\infty A^{-1} (3Ak + 4B'k^3) f dE. \quad (\text{A4})$$

Solving Eq. (A3) for  $k$  and substituting into Eq. (A4), we obtain

$$\int \nabla_{\mathbf{k}}^2 E f(E - E_F) d\mathbf{k} = \int_0^\infty \frac{3E^{\frac{1}{2}}}{A^{\frac{1}{2}}} \left[ 1 + \frac{5B'}{6A^2} E \right] dE. \quad (\text{A5})$$

By substituting Eq. (A3) into Eq. (A2) we find the carrier density:

$$N = \frac{1}{\pi^2} \int_0^\infty f \frac{E^{\frac{1}{2}}}{2A^{\frac{1}{2}}} \left( 1 - \frac{5B'}{2A^2} E \right) dE. \quad (\text{A6})$$

Equations (A5) and (A6) substituted into Eq. (11)

yield the reflectivity effective mass:

$$1/m_{\text{op}}^* = \frac{2A}{\hbar^2} \left[ 1 + \frac{10B'}{3A^2} \frac{\int_0^\infty kT x^{\frac{1}{2}} f(x - \eta) dx}{\int_0^\infty x^{\frac{1}{2}} f(x - \eta) dx} \right]. \quad (\text{A7})$$

The Faraday rotation per unit length can be calculated from the expression,<sup>21</sup>

$$\theta = \frac{Be^3}{8\pi^2 n \hbar^4 \epsilon_0 c \omega^2} \int \frac{\partial f(E - E_F)}{\partial E} \times \left[ \frac{\partial E}{\partial k_y} \frac{\partial^2 E}{\partial k_x \partial k_y} - \frac{\partial^2 E}{\partial k_y^2} \frac{\partial E}{\partial k_x} \right] \frac{\partial E}{\partial k_x} d\mathbf{k}, \quad (\text{A8})$$

which for spherical energy surfaces becomes

$$\theta = \frac{Be^3}{6\pi^2 n \hbar^4 \epsilon_0 c \omega^2} \int_0^\infty f(E - E_F) \times \left[ \left( \frac{dE}{dk} \right) + 2k \left( \frac{d^2 E}{dk^2} \right) \right] dE. \quad (\text{A9})$$

Substituting Eq. (A3) into Eq. (A9), we obtain

$$\theta = \frac{Be^3}{2\pi^2 n \hbar^4 \epsilon_0 c \omega^2} \int_0^\infty f A^{\frac{1}{2}} E^{\frac{1}{2}} \left( 1 + \frac{25B'}{6A^2} E \right) dE. \quad (\text{A10})$$

Equations (A10) and (A2) compared with Eq. (1) yield for the Faraday rotation effective mass the value given by Eq. (A7). The Faraday rotation effective mass has thus been shown to be identical with the reflectivity effective mass for energy bands of the form (A3). Substituting into Eq. (A7) the values of  $A$  and  $B$  found by expanding Eq. (4), Eq. (5) is found.

<sup>21</sup> M. J. Stephen and A. B. Lidiard, J. Phys. Chem. Solids **9**, 43 (1959).